Desalination and Water Treatment
www.deswater.com
doi: 10.1080/19443994.2014.975284

57 (2016) 1671–1683
January

Taylor & Francis
Taylor & Francis Group

Enhanced adsorptive removal of methylene blue from aqueous solution by soft rush (*Juncus effusus*)

Xingyu Liu*, Baoyan Wang, Zhixing Su

State Key Laboratory of Applied Organic Chemistry and Key Laboratory of Nonferrous Metal Chemistry and Resources Utilization of Gansu Province, College of Chemistry and Chemical Engineering, Lanzhou University, Lanzhou 730000, P.R. China, Tel. +86 0931 8912596; Fax: +86 0931 8912582; email: liuxingyu@lzu.edu.cn (X. Liu)

Received 2 September 2013; Accepted 4 October 2014

ABSTRACT

The adsorption of dye methylene blue by *Juncus effusus* has been investigated at 15, 25, and 35℃ temperatures. The influences of the uptake conditions were tested including the initial dye concentration, aqueous pH, and temperature. The adsorption kinetics was described by the different models, such as pseudo-first-order, the pseudo-second-order, and the Elovich. The results showed that the kinetic data were well described by the pseudo-second-order kinetic model. Thermodynamic parameters such as enthalpy change (ΔH), entropy change (ΔS), and free energy change (ΔG) were evaluated to predict the nature of adsorption. The calculated values of ΔH, ΔS, and ΔG for uptake of MB were 39.77 kJ/mol, 135.885 J/mol K, and −2.082 kJ/mol, respectively. This indicated the endothermic and spontaneous nature of the adsorption process. Linear form of Langmuir isotherm model can well agree with the experiment data, and the maximum adsorption capacity was found to be 117.93 mg/g at 35℃.

Keywords: Juncus effusus; Natural adsorbents; Methylene blue; Adsorption

1. Introduction

Water contamination due to dyes from the textile sources is a major environmental concern. During textile/leather processing, inefficiencies in dyeing result in a large amount of dyestuff being directly lost in the wastewater, which ultimately finds way into the environment. It is estimated that 10–35% of the dye is lost in the effluent during the dyeing process. The release of colored effluent wastewaters into the aquatic ecosystem represents both environmental and public health risks because of their negative ecotoxicological effects and bioaccumulation in wildlife. Such wastewater streams can be treated using suitable adsorbents, but creates potential disposal problems. Currently, there is no effective technology available for the removal of these toxic dyes from effluents [1–10].

Methylene blue (MB) (structure showed in Fig. 1), which is the most commonly used substance for dyeing cotton, wood, and silk. It can cause eye burns which may be responsible for permanent injury to the eyes of human and animals. Furthermore, they may be mutagenic, teratogenic, and carcinogenic and cause many health disorders to human beings such as dysfunction of the kidney, reproductive system, liver, brain, and central nervous system [11].

In recent years, various techniques have been developed for the removal of MB and its compounds from water and wastewater. These methods such as flocculation, reverse osmosis, and adsorption by

*Corresponding author.

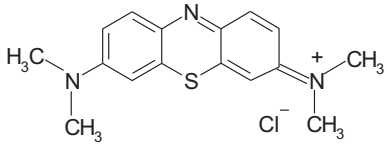

Fig. 1. Chemical structure of MB.

different materials have been used in wastewater treatment. Among them, adsorption has become one of the most effective methods. It is an effective technique for the treatment of wastewater containing dyes in terms of its initial cost, flexibility and simplicity of design, ease of operation, and insensitivity to toxic pollutants [12,13].

Juncus effusus (JS) is distributed in all parts of China, growing on wet lands or marsh edges. It is a rhizomatous perennial that can form monotonous standing as a result of both vigorous clonal growth and high seed production. Natural products soft rush JS is a porous material, which medulla, roots, and rhizome belong to the Juncaceae plants. It has a slender cylindrical with the diameter of 2–3 mm and the length of up to 120 cm. The surface of JS is white or light yellow with thin vertical lines. The chemical composition of JS contains a variety of phenanthrene derivatives, araban, xylan, methylpentosan, luteolin, and others [14,15].

JS contains abundant floristic fiber and some functional groups, which make the adsorption processes possible, such as carboxyl and hydroxy. JS is very light, and the rapid germination may result in very efficient colonization. In the past years, natural JS has been only explored as an effective adsorbent for the removal of various heavy metals [16,17]. But, the removal of dyes using JS as studied in this paper is seldom reported.

Therefore, in this work, JS were utilized as low-cost adsorbent to remove basic dye MB from aqueous solution by adsorption. The characteristic of adsorbent was measured. The influences of adsorption parameters such as pH, adsorbent concentration, contact time, and the initial dye concentration were also investigated. Finally, the applicability of various adsorption kinetic and isotherm models was tested.

2. Materials and methods

2.1. Chemical materials

The medicinal materials (JS) are mainly produced in Sichuan, Guizhou, Fujian, Gansu, etc. In this study, JS was obtained from Gansu, China. They were washed repeatedly with acetone and ethanol for several times to remove dirt particles and soluble impurities. JS were allowed to dry in an air oven at 40˚C for 2 d.

MB (C.I.52015), ≥98% dye content, was supplied by Shanghai Chemicals & Reagent Corp., China. All reagents were of analytical grade. The MB stock solution of 1 g/L concentration was prepared by dissolving an accurately weighed amount of MB in distilled water. The experimental solutions were obtained by diluting the dye stock solutions in accurate proportions to obtain different initial concentrations. The pH value of the test solutions was adjusted using the reagent grade sodium hydroxide (0.5 N) and the dilute hydrochloric acid (0.1 N).

2.2. Instruments

The surface functional groups of the natural JS and the adsorption interactions of dyes onto JS from aqueous solutions were investigated using Fourier transform infrared (FTIR) spectroscopy, FTIR were recorded on a Nicolet EXUS 670 FTIR spectrometer by dispersing samples in KBr disks. The concentrations of dye solutions were measured using Lambda 35 UV spectrometer (Perkin Elmer). The content of JS was measured by IRIS ER-S WP-1 plasma emission (ICP). The morphology of JS and JS-MB was observed by scanning electron microscopy (SEM) using a FEI Quanta 200 F field-emission electron microscope operated at 30 kV.

2.3. Experimental methods

A series of adsorption experiments of MB onto JS were carried out. The aqueous solutions of MB were prepared by adding the required quantity of JS slowly to distilled water with continuous stirring (400 rpm) using a magnetic stirrer at a certain temperature. The investigated parameters include pH of the adsorption medium, adsorbent dosage, contact time, the initial concentration, removal efficiency, and adsorption capacity. All experiments were carried out at 15˚C, 25˚C, and 35˚C, respectively.

After adsorption, the adsorbent was separated by filtering and the concentration of dyes in solution was determined on a UV–vis spectrophotometer at 665 nm. The obtained data were employed to develop equilibrium and kinetic mathematic models. All of the experimental data were the averages of triplicate determinations. The relative errors of the data were controlled within 5%.

3. Results and discussion

3.1. Characterization of JS and JS-MB

The chemical characteristics of the activated JS were determined by using standard analytical procedures [18]. It was found that in the analyzed JS sample, CaO, MgO, SiO_2, Na_2O, Fe_2O_3, MnO_2, BaO, and SrO were present 49.23, 13.65, 13.00, 10.22, 9.31, 3.36, 2.15, and 0.454% by weight, respectively [19].

The FTIR spectra analyses of JS and MB-adsorbed JS are shown in Fig. 2. FTIR study of JS confirms the defective sites at the surface of JS and the presence of –OH (3,432 cm^{-1}), C–H (2,923 cm^{-1}), –C=O (1,732 cm^{-1}), and C–O (1,634 cm^{-1}) functional groups at the surface of JS, which leads to the hydrophilic nature of JS. These functional groups may also act as anchoring sites for dye molecules [20]. The region below 1,000 cm^{-1} was the "fingerprint zone," and the absorption could not be clearly assigned to any particular vibration because they corresponded to complex interacting vibration systems [21].

After MB loading, there were some changes in some peaks. The wave number of –OH group blue shifted from 3,438 to 3,432 cm^{-1} compared with that of JS. From the IR spectra of JS-MB, it was shown that JS-MB led to the decrease in the adsorption band corresponding to the stretching vibration of the carboxyl group (at 1,715 cm^{-1}), which reflects the evidence of the strong interaction between MB and JS. The peak at 1,634 cm^{-1} almost did not change, but intensity of the peak was dramatically weakened. It indicated that MB might be easily adsorbed by JS through π–π stacking interactions and electrostatic attractions, as schematically illustrated in Fig. 2. In the spectrum of JS-MB, the new absorption peak at 1,603 cm^{-1} and the sharp peak at 1,331 cm^{-1} can be clearly observed, which can be assigned to the vibration of the aromatic ring and C–N bond for MB [22].

Hydroxyl and carboxyl groups may function as proton donors, and as a consequence, when deprotonated these groups may be involved in coordination with positive dye ions. Dissolved MB ions are positively charged and will undergo attraction on approaching the anionic JS structure by electrostatic forces. On this basis, it is expected that JS will show a strong sorption affinity toward MB ion. MB is also an ideally planar molecule and therefore can be easily adsorbed by JS through π–π stacking interactions between the aromatic backbone of the dye and phenanthrene derivatives of JS, which may lead to the weakening of the intensity of υ=CH for the JS-MB. The electrostatic attraction and π–π stacking interactions [23,24] between JS and MB could be responsible for the adsorption ability of the JS-MB.

3.2. SEM of JS, JS-MB, and JS-PANI

Fig. 3(a)–(c) shows SEM images of pure JS with different magnification and JS-PANI (JS-polyaniline,

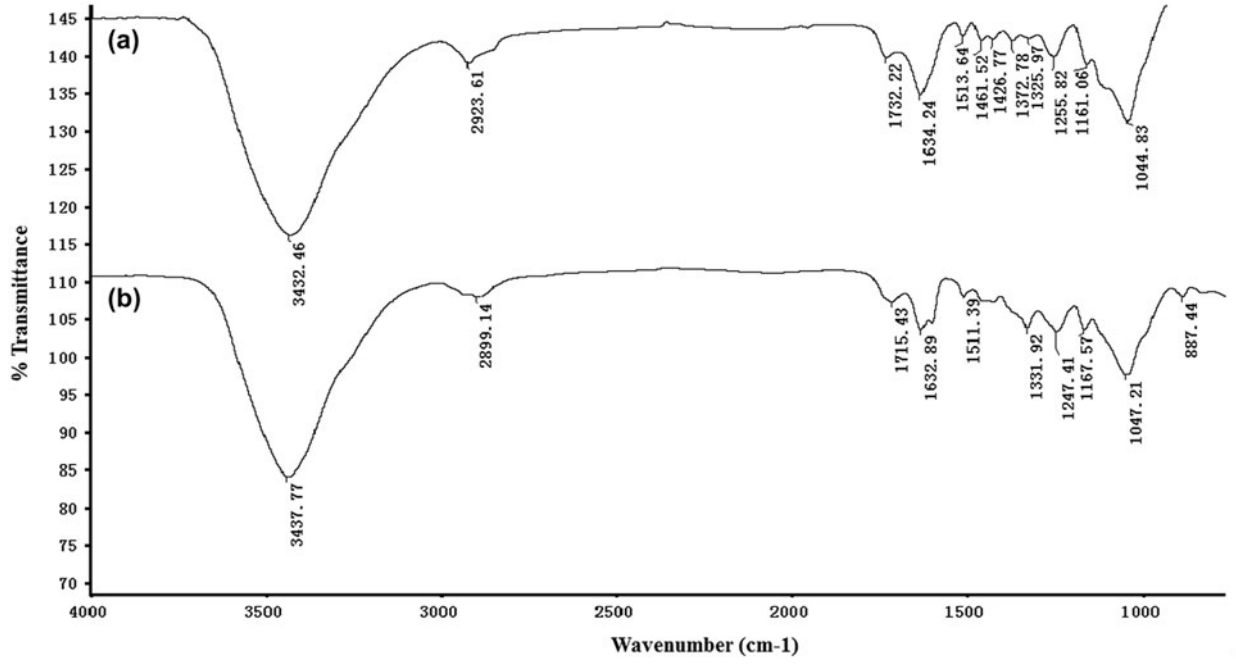

Fig. 2. Fourier transform infrared spectra of (a) JS and (b) JS-MB.

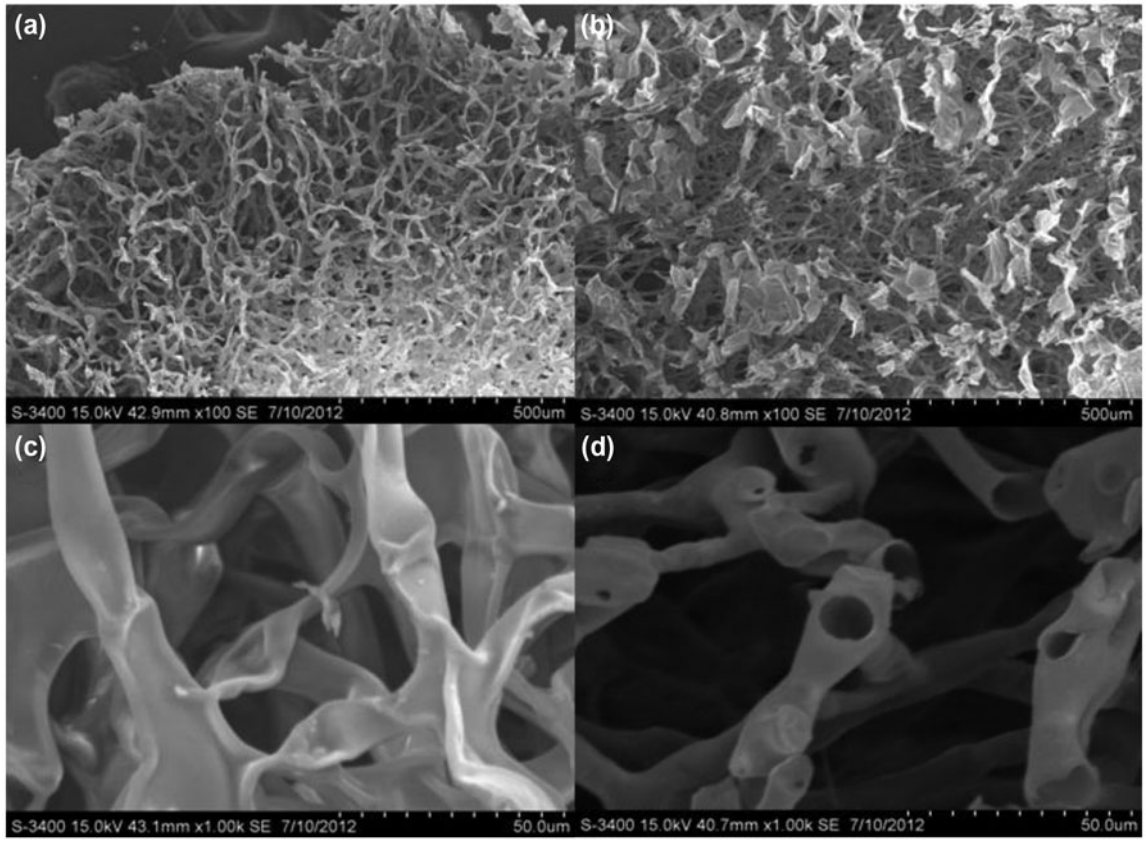

Fig. 3. SEM images of pure JS with low magnification (a and b), high magnification (c), and JS-PANI with high magnification (d).

Fig. 3(d)) prepared by *in situ* polymerization [25,26]. JS contains some carboxylic groups which would serve as reactive and anchoring sites for the interaction of polyaniline. Because of this mesopores structure, JS can provide active adsorption sites for the efficient removal of dye pollutes in water. These SEM images give some important information concerning the formation of tubes and pores. The representative JS in Fig. 3(c) shows that JS has some tubular structures and smooth surface. These tubes were mainly closed. In Fig. 3(d), the tubes of JS-PANI are mainly open and the sizes of holes are about 70–80 μm. The exposed surface can serve as an advanced adsorbent platform to remove the environmentally pollutant organic dyes. Fig. 4(a) shows the general view of JS-MB. After adsorption, the JS experienced an obvious structural change, many triangles and big apertures are generated on the cross section (Fig. 4(b)). The porous aerenchyma tissue [27] replicated in the JS-MB product is characterized by star-shaped cells with a strut thickness of 2–5 μm and a length of 300–600 μm (Fig. 4(c)). Based upon this hypothesis, we investigated the adsorption efficiency and mechanism of MB dye onto JS.

3.3. Kinetics and equilibrium of adsorption

3.3.1. Effect of initial pH

Initial pH value is one of the key variables in the adsorption process, where it could either increase or depress the adsorption equilibrium [28]. The pH of the dye solution affects not only the surface charge of the adsorbent, the degree of ionization of the materials, and the dissociation of functional groups on the active sites of the adsorbent, but also the structure of the dye molecule. Hence, five different pH values were used to determine their effects on the adsorption equilibrium in this study. Fig. 5(a) shows the effect of initial pH on the removal percentage of MB in the pH range of 7.75–12 at 15˚C with 42.93 mg/L of dye solution and 0.05 g/L of adsorbent. The maximum adsorption capacity, approximately 64.18 mg/g for MB, was achieved around pH 11. As a result, the initial pH value was optimized as 11 for dye removal [29].

As the pH of dye solution becomes higher, the association of dye cations with negatively charged functional groups in the adsorbent surface could more easily take place as follows [30,31]:

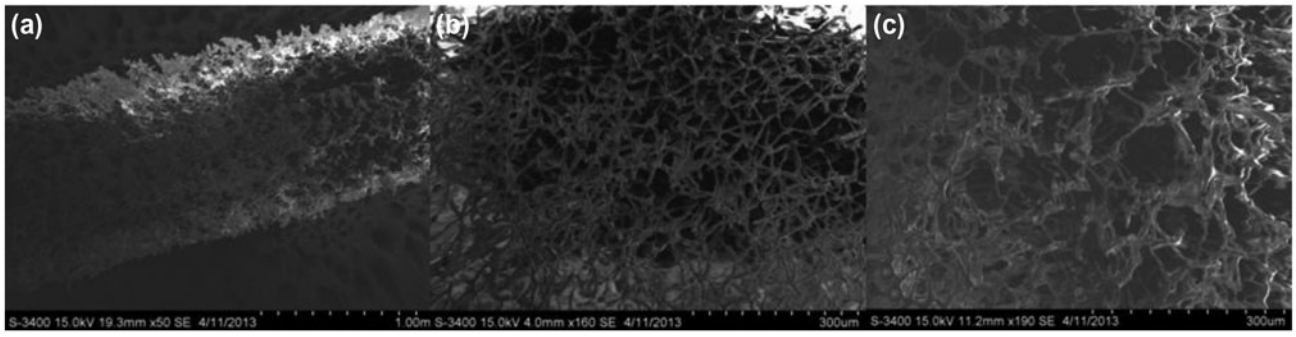

Fig. 4. SEM images of the MB-adsorbed JS with (a) low magnification and (b and c) high magnification.

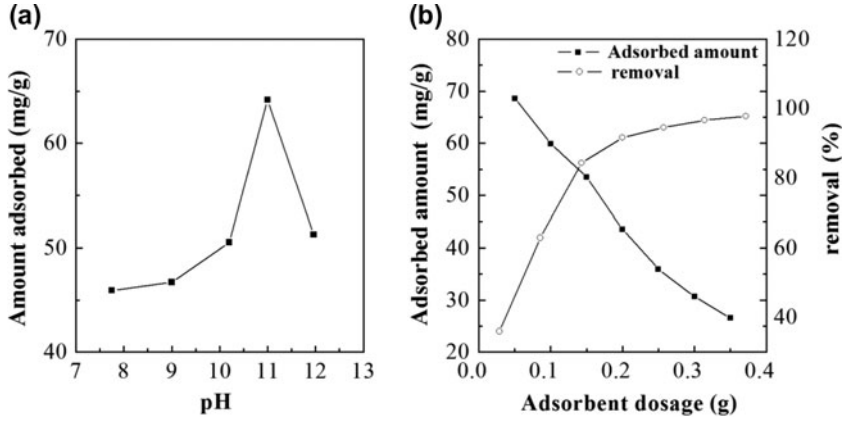

Fig. 5. Effect of initial pH (panel a) (initial conc. MB = 42.93 mg/L, JS conc. = 0.5 g/L) and of the adsorbent dose (panel b) (initial MB conc. = 100 mg/L, JS conc. = 1 g/L, pH 11) on the adsorption of MB by JS (T = 288 K, contact time: 24 h).

$$\text{JS–OH} + \text{OH}^- \rightarrow \text{JS–O}^- + \text{H}_2\text{O}$$
$$\text{JS–COOH} + \text{OH}^- \rightarrow \text{JS–COO}^- + \text{H}_2\text{O}$$

$$\text{JS–O}^- + \text{Dye}^+ \rightarrow \text{JS} - \text{O–Dye}$$
$$\text{JS–COO}^- + \text{Dye}^+ \rightarrow \text{JS–COO–Dye}$$

For JS, its main functional groups are the hydroxyl group and the carboxyl group. Along with an increase in the pH value, the concentration of H^+ ions that compete with the dye cations for sorption sites decreased. The increase in the solution pH was helpful for the adsorption of MB onto adsorbent. When the pH was low, the presence of excess H^+ ions could restrain the ionization of the carboxyl group. Therefore, the non-ionic form of the carboxyl group –COOH and the hydroxyl group –OH was present. The adsorption capacity of the dyes was low because of the absence of electrostatic interaction. When the pH was high, the carboxyl group and the hydroxyl group are turned into negatively charged such as $–COO^-$and $–O^-$, which may result in the increase in adsorption of cationic dye molecules due to the electrostatic attraction [32].

3.3.2. Effect of adsorbent dosage

The size and amount of adsorbent significantly influence the amount of MB adsorption. The surface area and adsorption capacity of each adsorbent significantly increased with increasing the amount of adsorbent [33].

The values of Q_e and the removal efficiency of dye (R%) at different dosage of JS were presented in Fig. 5(b). As the JS powder concentration increased from 0.5 to 3.5 g/L, the efficiency of adsorbed MB were increased from 36.04 to 97.78%. However, the adsorption capacity (Q_e) presented the opposite trend. The increase in the removal rate of dye was due to the increased adsorbent surface area and the availability of more adsorption sites. The decrease of Q_e from 68.6 to 26.59 mg/g with increasing adsorbent concentration

from 0.5 to 3.5 g/L was attributed to the adsorption competition among adsorbent and the split in the concentration gradient [32]. When the concentration of JS powder was 1.5 g/L, the Q_e and $R\%$ were 53.5 mg/g and 84.31%, respectively. Above 1.5 g/L of adsorbent dosage, there was no significant increase in the removal rate of dye, but the Q_e decreased rapidly. Considering Q_e and $R\%$, adsorbent dosage of 1.5 g/L was found to be the optimum concentration for all other batch experiments.

3.3.3. Effect of contact time and of the initial concentration on the uptake of MB

The initial concentration of the dye is an important driving force to overcome the mass transfer resistance of the dye from the aqueous and the solid phase. The effect of contact time on the adsorption of MB onto JS is shown in Fig. 6 for a fixed initial dye concentration 42.93, 65.44, 82.68, and 95.98 mg/L for MB and pH 11 at 15℃.

As can be seen in Fig. 6, the overall trend was an increase in the adsorption capacity on increasing the dye concentration. It was observed that dye uptake was rapid from the beginning of the experiment and thereafter, it proceeded at a slower rate and finally reached saturation. With the increase in concentration, the trend becomes more obvious. This highlights the strong chemical interaction between the dye molecules and JS [34].

3.3.4. Adsorption kinetics

Adsorption is a physicochemical process that involves mass transfer of a solute from liquid phase to the adsorbent surface. In order to investigate the mechanism of dye adsorption onto JS, three kinetic models were studied: pseudo-first-order, pseudo-second-order, and Elovich. These models are the most used to describe dye and other pollutants adsorption such as dyes onto solid adsorbents [35].

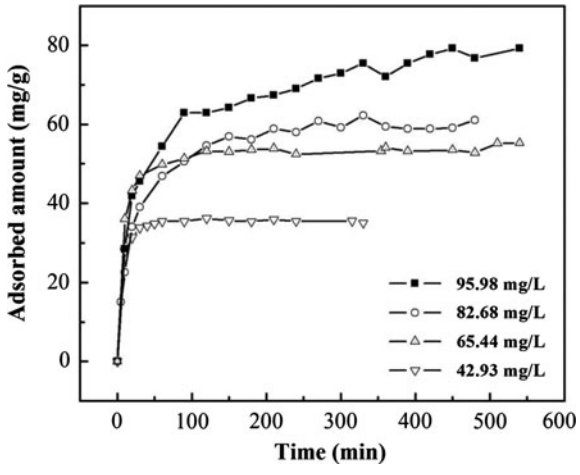

Fig. 6. Effect of contact time on the adsorption of MB onto JS at different dye concentrations (JS conc. = 1 g/L, pH 11, T = 298 K).

3.3.4.1. Pseudo-first-order and pseudo-second-order models. The linear form of pseudo-first-order rate equation is [36]:

$$\log(Q_e - Q_t) = \log Q_e - \frac{k_{ad}t}{2.303} \quad (1)$$

where Q_e and Q_t are the amounts of MB adsorbed (mg/g) at equilibrium and time t (min), respectively; k_{ad} is the rate constant of the pseudo-first-order kinetic model (min^{-1}).

A linear form of pseudo-second-order kinetic model is expressed by the following equation:

$$\frac{t}{Q_t} = \frac{t}{Q_e} + \frac{1}{h} \quad (2)$$

The initial adsorption rate h (mg/g min) at $t = 0$ is defined as follows:

$$h = k_2 Q_e^2 \quad (3)$$

where k_2 is the rate constant (g/mg min) of pseudo-second-order kinetic model for adsorption [37]. The intercept of the plots of t/Q_t vs. t was used to calculate the rate constant k_2 and the initial adsorption rate h.

3.3.4.2. The Elovich model. The Elovich model is useful for energetically heterogeneous solid surfaces and is given in the following equation [38]:

$$Q_t = \frac{1}{\beta}\ln(\alpha\beta) + \frac{1}{\beta}\ln t \quad (4)$$

where α (mg/g min) is the initial sorption rate and β (g/mg) is related to the extent of surface coverage and the activation energy for chemisorption. If MB adsorption onto JS fits the Elovich model, plots of Q_t vs. ln (t) should give a linear relationship with a slope of ($1/\beta$) and an intercept of ($1/\beta$) ln ($\alpha\ \beta$).

Pseudo-first-order, pseudo-second-order, and Elovich models have been used to fit experimental data obtained from batch MB removal experiments. To explore the adsorption kinetics of MB on JS, Fig. 7 presents the fitting of the experimental data to kinetic

models (lines). The linearized plots are shown in Fig. 7 as the inset, and the fitting results are listed in Table 1. Judging from R^2 values, we can see that the pseudo-second-order model gives the better fitting result in all cases. Because the pseudo-second-order model is based on the assumption that chemical sorption is the rate-determining step, the above results further support the proposed chemisorption mechanism for the systems. This suggests that the present adsorption process should be a chemisorption process involving exchange or sharing of electrons between the dye cations and functional groups of JS.

3.4. Adsorption isotherms

Adsorption isotherm models provide the useful data for understanding the mechanisms of the adsorption process and describe how an adsorbate interacts with an adsorbate and to evaluate the applicability of the process. The parameters and correlation coefficients obtained from the plots of Langmuir, Freundlich, Tempkin, and D–R (shown in Fig. 8) are listed in Table 2. They are different in the basic assumptions, shape of the isotherm, and nature of the adsorbent surface. They were helpful to determine the maximum adsorption capacity of adsorbate for the given adsorbent.

3.4.1. Langmuir model

The linearized form of the Langmuir adsorption isotherm equation (Eq. (5)) is [39]:

$$\frac{C_e}{Q_e} = \frac{1}{bQ_m} + \frac{C_e}{Q_m} \tag{5}$$

where C_e is the equilibrium concentration of the dye in the solution (mg/L), Q_e is the amount of the dye

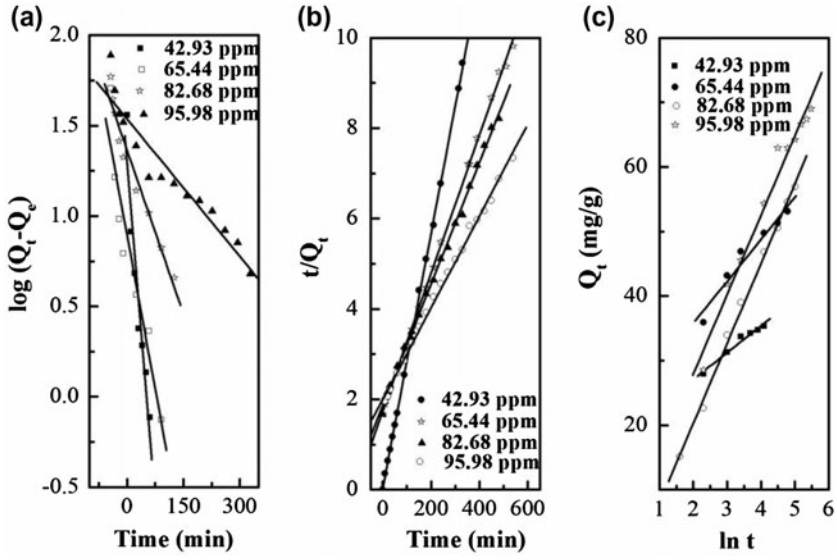

Fig. 7. Kinetic models for adsorption of MB onto JS: (a) pseudo-first-order, (b) pseudo-second-order, and (c) Elovich plot (JS conc. = 1 g/L, pH 11, T = 298 K, contact time: 24 h).

Table 1
Kinetic parameters for adsorption of MB onto JS

C_0 ppm	Q_e Exp.	Pseudo-first-order			Pseudo-second-order			Elovich		
		$k_{ad} \times 10^3$	Q_e	R^2	$k_2 \times 10^3$	Q_e	R^2	α	β	R^2
42.93	36.14	5.735	19.708	0.9611	25.5	35.45	0.99978	384.40	0.2410	0.9856
65.44	54.08	2.819	26.594	0.9543	1.75	55.96	0.99985	214.542	0.1536	0.9763
82.68	60.84	1.51	45.532	0.9790	1.12	61.996	0.99912	8.6372	0.0808	0.9978
95.98	81.06	0.631	47.373	0.9557	0.061	82.78	0.99946	17.4385	0.0835	0.9917

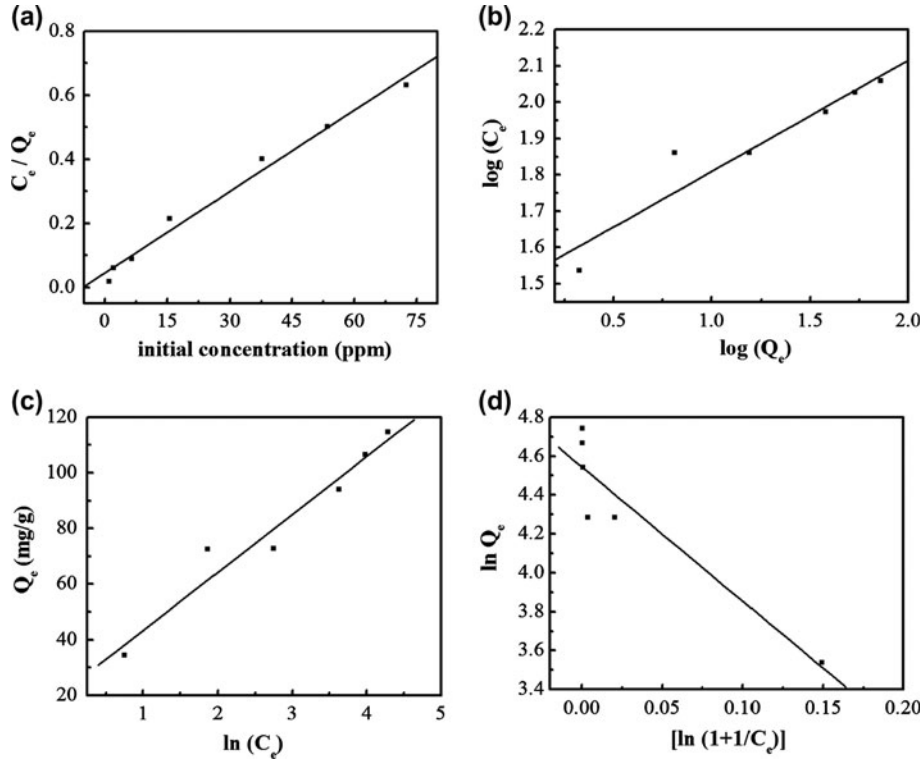

Fig. 8. Various adsorption isotherms for the adsorption of MB dye onto JS (JS conc. = 1 g/L, pH 11, T = 308 K, contact time: 24 h).

adsorbed per unit mass of adsorbent (mg/g), Q_m [$Q_m = K_L/b$] signifies the maximum adsorption capacity (mg/g), which depends on the number of adsorption sites, and b (L/mg) and K_L (L/g) are the Langmuir constants with b being related to the adsorption energy. The values of b and K_L were calculated from the slope and intercept of the plot of C_e/Q_e vs. C_e.

Furthermore, the effect of the isotherm shape was studied to understand whether an adsorption system is favorable or not. Another important parameter, R_L, [40] called the separation factor or equilibrium parameter, which can be used to determine the feasibility of adsorption in a given concentration range over adsorbent, was also evaluated from the relation.

$$R_L = \frac{1}{1 + bC_0} \tag{6}$$

where b is the Langmuir adsorption constant (L/mg) and C_0 is the initial dye concentration (36.5–187 mg/L). Ho and McKay [41] established that (1) $0 < R_L < 1$ for favorable adsorption; (2) $R_L > 1$ for unfavorable adsorption; (3) $R_L = 1$ for linear adsorption; and (4) $R_L = 0$ for irreversible adsorption. The value of R_L for MB adsorption onto JS ranges between 0.0278 and 0.1279 (Table 2), confirming the favorable uptake of the dye. Namely, Langmuir model could simulate the adsorption equilibrium data of the dye in the concentration range studied (35–115 mg/g).

3.4.2. Freundlich model

The Freundlich model is another model which has the following form [42]:

$$\log Q_e = \log K_f + \frac{1}{n} \log C_e \tag{7}$$

where Q_e is the amount of dye adsorbed per gram of adsorbent (mg/g); C_e is the equilibrium dye concentration in solution (mg/L); K_f and n are the Freundlich constants, which represent the adsorption capacity and the adsorption strength, respectively. The magnitude of $1/n$ quantifies the favorability of adsorption and the degree of the adsorbent surface heterogeneity.

The Freundlich constant ($1/n$) is related to the sorption intensity of the sorbent. When $0.1 < 1/n \leq 0.5$, it is easy to adsorb; if $0.5 < 1/n \leq 1$, there are some difficulties with the absorption; if $1/n > 1$, it is quite

Table 2
Isotherm parameters for the adsorption of MB onto JS

Isotherm models	Parameters	Value	R^2
Langmuir	Q_m	117.93 mg/g	0.9928
	b	0.187 L/mg	
	K_L	22.053	
	R_L	0.0278–0.1279	
Freundlich	K_f	31.90 L/mg	0.9528
	$1/n$	0.30616	
Tempkin	A_T	1.0492 L/g	0.9745
	B_T	15.545	
	b_T	122.872 J/mol	
Dubinin–Radushkevich	Q_m	94.13 mg/g	0.9371
	$K \times 10^{-6}$	1.05	
	E	0.689 kJ/mol	

difficult to adsorb [19]. The results are listed in Table 2. The $1/n$ and K_f values of MB on JS were 0.30616 and 31.90 L/mg, respectively, indicating that the dye could be easily adsorbed on the JS and the JS exhibited a high adsorption capacity for the target organic dye [43,44]. The Freundlich expression is an empirical equation based on adsorption at a heterogeneous surface. The results indicated that the linear correlation coefficients for Langmuir and Freundlich models were 0.9928 and 0.9528, respectively, which indicated that the experimental data well correlated with the two equations. Furthermore, Langmuir isotherm model showed a better fit with adsorption data than Freundlich isotherm model. The high correlation coefficient ($R^2 > 0.99$) shows that Langmuir isotherms are applicable for the interpretation of MB adsorption onto JS over the whole concentration range studies and maximum adsorption capacity of 117.93 mg/g for JS. The Langmuir isotherm model assumes that (i) a monolayer adsorption should exist on the adsorbent surface with a finite number of identical sites; (ii) all sites are energetically equivalent; and (iii) there is no interaction between the adsorbed molecules. Whereas in the Langmuir theory, the basic assumption is that the sorption takes place at specific homogeneous sites within the adsorbent.

3.4.3. Tempkin model

Tempkin isotherm contains a factor that explicitly takes into the account of adsorbing species–adsorbent interactions. It assumes that (i) the adsorption is characterized by a uniform distribution of binding energies and (ii) the heat of adsorption of all the molecules in the layer decreases linearly with coverage due to adsorbent–adsorbate interactions. Tempkin isotherm has generally been used in the linearized and rearranged form as shown by the following equation [45]:

$$Q_e = B_T \ln A_T + B_T \ln C_e \tag{8}$$

where $B_T = RT/B_T$ and A_T are the equilibrium binding constants corresponding to the maximum binding energy (L/g), B_T is the Tempkin constant related to the heat of adsorption, T is the absolute temperature in Kelvin, and R is the universal gas constant. The Tempkin constants A_T and B_T can be determined from the slope and intercept of Q_e vs. ln C_e (Table 2).

3.4.4. Dubinin–Radushkevich (D–R) Model

The D–R isotherm model has the following form:

$$\ln Q_e = \ln Q_m - K\varepsilon^2 \tag{9}$$

where Q_e is the amount of dye adsorbed per unit mass of adsorbent (mg/g), Q_m is the theoretical saturation capacity (mg/g), K is a constant related to the mean free energy of adsorption (mol^2/kJ^2), and ε is the Polanyi potential which is equal to

$$\varepsilon = RT \ln\left(1 + \frac{1}{C_e}\right) \tag{10}$$

The mean free energy of adsorption (E), defined as the free energy change when one mole of ion is transferred from infinity in solution to the surface of the solid, was calculated from the K value using the following relation [46]:

$$E = \frac{1}{\sqrt{-2K}} \tag{11}$$

On the basis of Eqs. (9)–(11), the isotherm constants, E, and the determination coefficients were calculated.

The values of the Tempkin parameters were found to be A_T (1.049 L/g) and B_T (15.545). The Tempkin constant B_T (122.87 J/mol) that is related to heat of sorption indicates physiochemical nature of the sorption process. The adsorption parameter K of Dubinin–Radushkevich (D–R) isotherm gives the mean free energy (E) of sorption per molecule of the adsorbate when it is transferred to the surface of the solid from infinity in the solution. The apparent energy of adsorption E can judge adsorption process as physical or chemical. A sorption process is generally considered as physical if $E \leq 8$ kJ/mol, and as chemical when E value lies between 8 and 16 kJ/mol [47]. The apparent energy of adsorption, E (0.689 kJ/mol), indicated a physisorption process. The value of correlation coefficient (0.975) indicated that the Tempkin isotherm gave a good fit to the sorption process.

The experimental data of these isotherms summarized in Table 2 show that the Langmuir model and the Tempkin model yielded the better fit with the higher R^2 values as compared to the other models. And it showed that the Langmuir isotherm gave the best fits than the other isotherms. So it illustrated that the adsorption on the surface of JS was a monolayer adsorption. According to the Langmuir equation, the maximum uptake capacity (Q_m) for MB was 117.93 mg/g. Therefore, the adsorption of MB by JS was regarded as physical adsorption combined with the effect of chemical adsorption.

Previously, some researchers investigated several adsorbents for the removal of MB from aqueous solutions. Table 3 makes such a comparison with other biomass based on the adsorbents and shows that JS is advantageous over many adsorbents reported in the literature [21,22,48–55].

3.5. Effect of temperature and thermodynamic analysis

The adsorption experiments were carried out at 15, 25, and 35°C in order to investigate the effects of temperature on the adsorption of MB onto JS. The removal of MB by adsorption onto JS increases from 66.18 to 117.93 mg/g when the temperature was increased from 15 to 35°C. Fig. 9 indicated that the adsorption process of dye cations was endothermic in nature. It is well known that the diffusion rate of the adsorbate molecules across the external boundary layer and in the internal pores of adsorbent particles increases and viscosity of the aqueous solution decreases by increasing the temperature of the adsorption medium [53].

The data obtained from the temperature study were used for thermodynamic analysis. Thermodynamics analysis was focused on the Gibbs free energy, which is presented in Eq. (12). The Gibbs free energy can also be expressed using enthalpy and entropy at a constant temperature (Eq. (13)). The linearized form of Eqs. (12) and (13) results in Eq. (14), which is the van't Hoff equation [33]:

$$\Delta G = -RT \ln K_d \tag{12}$$

$$\Delta G = \Delta H - \Delta S \tag{13}$$

$$\ln K_d = \frac{\Delta S}{R} - \frac{\Delta H}{RT} \tag{14}$$

In MB adsorption, ΔS (J/mol K) is the entropy change of MB adsorption, R is the universal gas constant (8.314 J/mol K), T is the absolute temperature (K), and K_d is the Langmuir constant. ΔH and ΔS were calculated from the slope and intercept of the van't Hoff plot of ln K_d vs. $1/T$, respectively.

Table 3
Reported maximum adsorption capacities (Q_m) in the literature for MB dye obtained on various biomass-based adsorbents

Adsorbent	Adsorption capacity (mg/g)	Reference
Peanut husk	72.13 ± 3.03	[21]
Activated carbon of rice husk	9.73	[48]
Modified *Ficus carica*	75.87	[49]
Pine cone biomass	109.89	[50]
Cashew nut shell	5.184	[51]
Oxalic acid modified rice husk	19.77–53.21	[52]
Almond shell (*Prunus dulcis*)	51.02	[53]
Wheat straw	60.66	[54]
Spent rice biomass	8.30	[55]
Silkworm exuviae	26.6	[22]
Juncus effusus	117.93 ± 2.14	This work

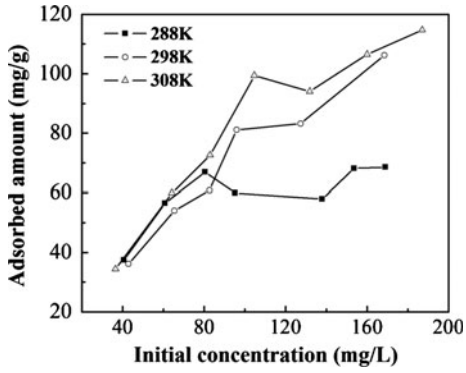

Fig. 9. Effect of temperature on the uptake of MB by JS (initial pH 11, JS conc. = 1 g/L, contact time: 24 h).

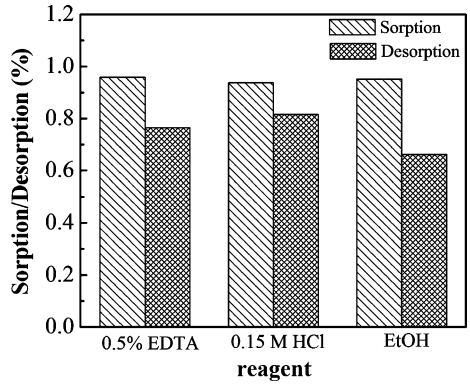

Fig. 10. MB adsorption–desorption cycles with 0.5% EDTA or 0.15 M HCl or ethanol as desorbing agent.

As can be seen in Table 4, ΔH was positive value, implying endothermic reaction. The positive value of ΔS suggested that the increased randomness occurs at the solid and solution interface during the adsorption of MB onto JS. The negative ΔG value indicated that the process be feasible and possess the spontaneous nature of adsorption. Furthermore, the decrease in the values of ΔG with the increasing temperature revealed the adsorption was more spontaneous at higher temperatures [56].

3.6. Desorption of dye

Adsorbent of 0.05 g was treated with 20 mg/L MB solution at 303 K for 24 h at pH 11. The mixture was filtered, and the filtrate was analyzed for amount of dye adsorbed using UV–visible spectrophotometer.

The MB loaded adsorbent was washed with 0.5% EDTA or 0.15 M HCl or ethanol to remove unabsorbed dye. The results of desorption study was shown in Fig. 10. It clearly exhibits that MB has an extremely good desorption toward JS in the acidic medium, while in ethanol desorption is feeble. It has been observed that percentage adsorption of MB onto adsorbent is 93.72% at optimized conditions and percentage recovery for first cycle was 81.6% in 0.15 M HCl. The high desorption in acidic medium showed that the adsorption of MB onto adsorbent was mainly controlled by electrostatic attractions, which was in agreement with the results obtained previously.

Desorption studies help decide the mechanism of the adsorption process and recovery of adsorbent for reuse. If the dye adsorbed onto the adsorbent can be recovered by distilled water, it indicates that dye is attached to adsorbent by weak bonds. If the strong basic or acidic medium is used to recover the dye then adsorption occurs through ion exchange. As the regenerated adsorbent illustrated satisfactory adsorption capability toward MB dye, it can be used as a potential adsorbent for wastewater treatment [33].

3.7. Adsorption mechanism

The adsorption mechanism for dye removal by adsorption using an adsorbent material can be attributed to the multiple adsorption interaction mechanisms. The FTIR spectrum of the adsorbent indicates that carboxyl and hydroxyl groups are present in abundance. The sorption of MB on the adsorbent may be due to the electrostatic attraction between these groups and the cationic dye molecules. In addition, the FTIR spectra analysis indicated that MB might be easily adsorbed through JS by π–π stacking interactions. Those SEM images give important information concerning the formation of tubes and pores in JS and JS-MB, which can be explained as that mesopores may be favor to the adsorbate–adsorbate interaction via mesopore-filling mechanism. Dye transfer from the exterior surface of

Table 4
Thermodynamic parameters for the adsorption of MB onto JS

Temperature (K)	K_d (L/mol)	R^2	ΔH (kJ/mol)	ΔS (J/mol K)	ΔG (kJ/mol)
288	0.682	0.9320	39.77	135.885	0.636
298	1.706				−0.723
308	1.989				−2.082

the adsorbent to the interior pores of the particle through a pore diffusion or intra-particle diffusion mechanism [23,35].

4. Conclusions

Results presented in this paper showed that the adsorption capacity increased with the increase in the initial MB concentration, aqueous pH, and temperature. Thermodynamic analysis proved that MB adsorption onto JS is an endothermic process and is spontaneous in nature. The kinetics of MB adsorption onto adsorbent follows the pseudo-second-order model. The equilibrium data for JS was fitted well by the Langmuir isotherm model of adsorption, showing monolayer coverage of MB molecules at the surface of tubes and pores. The maximum sorption capacities of MB for JS were 66.18, 106.38, and 117.93 mg/g, respectively at 15, 25, and 35°C and pH 11. The electrostatic attraction and π–π stacking interactions between JS and MB account for the high adsorptive performance of the JS. Our adsorption results suggested that the JS could be employed as efficient and suitable adsorbent for the removal of MB dye from wastewater.

Acknowledgment

Financial support from the Fundamental Research Funds for the Central Universities of China (No. lzujbky-2013-195) is gratefully acknowledged.

References

[1] A. Mittal, V. Thakur, V. Gajbe, Adsorptive removal of toxic azo dye Amido Black 10B by hen feather, Environ. Sci. Pollut. Res. 20 (2013) 260–269.
[2] R. Jain, S. Sikarwar, Adsorptive removal of Erythrosine dye onto activated low cost de-oiled mustard, J. Hazard. Mater. 164 (2009) 627–633.
[3] R. Jain, V.K. Gupta, S. Sikarwar, Adsorption and desorption studies on hazardous dye Naphthol Yellow S, J. Hazard. Mater. 182 (2010) 749–756.
[4] V.K. Gupta, R. Jain, A. Mittal, T.A. Saleh, A. Nayak, S. Agarwal, S. Sikarwar, Photo-catalytic degradation of toxic dye amaranth on TiO_2/UV in aqueous suspensions, Mater. Sci. Eng. C 32(1) (2012) 12–17.
[5] J. Mittal, D. Jhare, H. Vardhan, A. Mittal, Utilization of bottom ash as a low-cost sorbent for the removal and recovery of a toxic halogen containing dye eosin yellow, Desalin. Water Treat. 23(1) (2013) 1–12.
[6] V.K. Gupta, I. Ali, T.A. Saleh, A. Nayak, S. Agarwal, Chemical treatment technologies for waste-water recycling—An overview, RSC Adv. 2 (2012) 6380–6388.
[7] V.K. Gupta, A. Mittal, D. Jhare, J. Mittal, Batch and bulk removal of hazardous colouring agent Rose Bengal by adsorption techniques using bottom ash as adsorbent, RSC Advances 2 (2012) 8381–8389.
[8] J. Mittal, V. Thakur, A. Mittal, Batch removal of hazardous azo dye Bismark Brown R using waste material hen feather, Ecol. Eng. 60 (2013) 249–253.
[9] K. Kandori, M. Oketani, M. Wakamura, Effects of Ti (IV) substitution on protein adsorption behaviors of calcium hydroxyapatite particles, Colloids Surf., B 101 (2013) 68–73.
[10] Z.Y. Zhang, I.M. O'Hara, G.A. Kent, W.O.S. Doherty, Comparative study on adsorption of two cationic dyes by milled sugarcane bagasse, Ind. Crops Prod. 42 (2013) 41–49.
[11] M. Rafatullah, O. Sulaiman, R. Hashim, A. Ahmad, Adsorption of methylene blue on low-cost adsorbents: A review, J. Hazard. Mater. 177 (2010) 70–80.
[12] S. Sohrabnezhad, A. Pourahmad, Comparison absorption of new methylene blue dye in zeolite and nanocrystal zeolite, Desalination 256 (2010) 84–89.
[13] K. Kandori, M. Oketani, M. Wakamura, Effects of Ti (IV) substitution on protein adsorption behaviors of calcium hydroxyapatite particles, Colloids Surf., B 101 (2013) 68–73.
[14] X.Y. Wang, C.Q. Ke, C.P. Tang, D. Yuan, Y. Ye, 9,10-Dihydrophenanthrenes and phenanthrenes from *Juncus setchuensis*, J. Nat. Prod. 72 (2009) 1209–1212.
[15] Medicinal Plant Images Database, School of Chinese Medicine (Latin Name: Juncus effuses L.). Available from: http://library.hkbu.edu.hk /electronic/libdbs/mpd/index.html.
[16] L.H. Zhing, Y. Li, P.R. Tong, Preparation of xanthogenate by modifying common rush residues for removing lead from propolis, J. Xi'an Polytech. Univ. 25 (2011) 503–504.
[17] S.D. Huang, Y.Y. Yang, B. Len, J. Qian, Y. Ren, G.W. Li, Z.H. Ren, An experimental study on wastewater treatment using constructed wetland plants, Sichuan Environ. 14 (1995) 5–7.
[18] A.I. Vogel (Ed.), Vogel's Textbook of Quantitative Chemical Analysis, fifth ed., Longman, London, 1989.
[19] H. Daraei, A. Mittal, M. Noorisepehr, F. Daraei, Kinetic and equilibrium studies of adsorptive removal of phenol onto eggshell waste, Environ. Sci. Pollut. Res. 20 (2013) 4603–4611.
[20] J. Sánchez-Martín, M. González-Velasco, J. Beltrán-Heredia, J. Gragera-Carvajal, J. Salguero-Fernández, Novel tannin-based adsorbent in removing cationic dye (Methylene Blue) from aqueous solution. Kinetics and equilibrium studies, J. Hazard. Mater. 174 (2010) 9–16.
[21] J.Y. Song, W.H. Zou, Y.Y. Bian, F.Y. Su, R.P. Han, Adsorption characteristics of methylene blue by peanut husk in batch and column modes, Desalination 265 (2011) 119–125.
[22] H. Chen, J. Zhao, G.L. Dai, Silkworm exuviae—A new non-conventional and low-cost adsorbent for removal of methylene blue from aqueous solutions, J. Hazard. Mater. 186 (2011) 1320–1327.
[23] J. Ma, F. Yu, L. Zhou, L. Jin, M.X. Yang, J.S. Luan, Y.H. Tang, H.B. Fan, Z.W. Yuan, J.H. Chen, Enhanced adsorptive removal of methyl orange and methylene blue from aqueous solution by alkali-activated multiwalled carbon nanotubes, ACS Appl. Mater. Interfaces 4 (2012) 5749–5760.
[24] L.H. Ai, C.Y. Zhang, F. Liao, Y. Wang, M. Li, L.Y. Meng, J. Jiang, Removal of methylene blue from aqueous solution with magnetite loaded multi-wall carbon

nanotube: Kinetic, isotherm and mechanism analysis, J. Hazard. Mater. 198 (2011) 282–290.
[25] M. Oh, S.J. Park, Y.J. Jung, S. Kim, Electrochemical properties of polyaniline composite electrodes prepared by *in situ* polymerization in titanium dioxide dispersed aqueous solution, Synth. Met. 162 (2012) 695–701.
[26] H.F. Su, T. Wang, S.Y. Zhang, J.J. Song, C.J. Mao, H.L. Niu, B.K. Jin, J.Y. Wu, Y.P. Tian, Facile synthesis of polyaniline/TiO_2/graphene oxide composite for high performance supercapacitors, Solid State Sci. 14 (2012) 677–681.
[27] K. Gutbrod, P. Greil, C. Zollfrank, Carbon auto-doping improves photocatalytic properties of biotemplated ceramics, Appl. Catal., B 103 (2011) 240–245.
[28] M. Constantin, I. Asmarandei, V. Harabagiu, L. Ghimici, P. Ascenzi, G. Fundueanu, Removal of anionic dyes from aqueous solutions by an ion-exchanger based on pullulan microspheres, Carbohydr. Polym. 91 (2013) 74–84.
[29] L.H. Ai, M. Li, L. Li, Adsorption of Methylene Blue from aqueous solution with activated carbon/cobalt ferrite/alginate composite beads: Kinetics, isotherms, and thermodynamics, J. Chem. Eng. Data 56 (2011) 3475–3483.
[30] R. Rakhshaee, M. Panahandeh, Stabilization of a magnetic nano-adsorbent by extracted pectin to remove methylene blue from aqueous solution: A comparative studying between two kinds of cross-likened pectin, J. Hazard. Mater. 189 (2011) 158–166.
[31] P. Bradder, S.K. Ling, S.B. Wang, S.M. Liu, Dye adsorption on layered graphite oxide, J. Chem. Eng. Data 56 (2011) 138–141.
[32] X.L. Han, W. Wang, X.J. Ma, Adsorption characteristics of methylene blue onto low cost biomass material lotus leaf, Chem. Eng. J. 171 (2011) 1–8.
[33] V.K. Gupta, D. Pathania, S. Agarwal, S. Sharma, Decoloration of hazardous dye from water system using chemically modified *Ficus carica* adsorbent, J. Mol. Liq. 174 (2012) 86–94.
[34] M. Auta, B.H. Hameed, Modified mesoporous clay adsorbent for adsorption isotherm and kinetics of methylene blue, Chem. Eng. J. 198–199 (2012) 219–227.
[35] K. Guimarães Gusmão, L. Alves Gurgel, T. Sacramento Melo, L. Gil, Application of succinylated sugarcane bagasse as adsorbent to remove methylene blue and gentian violet from aqueous solutions—Kinetic and equilibrium studies, Dyes Pigm. 92 (2012) 967–974.
[36] S. Lagergren, Zur theorie der sogenennten adsorption geloster stoffe (About the theory of so called adsorption of soluble substances), Kungliga Svenska Vetenskapsakademiens, Handlingar 24 (1898) 1–39.
[37] V.A. Cardoso, A.G. Souza, P.P.C. Sartoratto, The ionic exchange process of cobalt, nickel and copper(II) in alkaline and acid-layered titanates, Colloids Surf., A 248 (2004) 145–149.
[38] C.W. Cheung, J.F. Porter, G. Mckay, Sorption kinetic analysis for the removal of cadmium ions from effluents using bone char, Water Res. 35 (2001) 605–612.
[39] I. Langmuir, The constitution and fundamental properties of solids and liquids. Part I. solids, J. Am. Chem. Soc. 38 (1916) 2221–2295.
[40] K.R. Hall, I.C. Eagleton, A. Acrivos, T. Vermeule, Pore-solid-diffusion kinetics in fixed-bed adsorption under constant pattern conditions, Ind. Eng. Chem. Res. 5 (1966) 212–223.
[41] Y.S. Ho, G. McKay, Sorption of dye from aqueous solution by peat, Chem. Eng. J. 70 (1998) 115–124.
[42] H.M.F. Freundlich, Über die adsorption in lösungen (Over the adsorption in solution), Zeitschrift für Physikalische Chemie, Leipzig (J. Phys. Chem.), 57A (1906) 385–470.
[43] G. Walker, L. Weatherley, Adsorption of dyes from aqueous solution—The effect of adsorbent pore size distribution and dye aggregation, Chem. Eng. J. 83 (2001) 201–206.
[44] Q.H. Wu, C. Feng, C. Wang, Z. Wang, A facile one-pot solvothermal method to produce superparamagnetic graphene–Fe_3O_4 nanocomposite and its application in the removal of dye from aqueous solution, Colloids Surf., B 101 (2013) 210–214.
[45] M.J. Tempkin, V. Pyzhev, Kinetics of ammonia synthesis on promoted iron catalysis, Acta Physiochim. URSS 12 (1940) 327–356.
[46] J.P. Hobson, Physical adsorption isotherms extending from ultrahigh vacuum to vapor pressure, J. Phys. Chem. 73 (1969) 2720–2727.
[47] F. Helfferich, Ion Exchange, McGraw-Hill, New York, NY, 1962.
[48] Y.C. Sharma, Uma, S.N. Upadhyay, An economically viable removal of methylene blue by adsorption on activated carbon prepared from rice husk, Can. J. Chem. Eng. 89 (2011) 377–383.
[49] V.K. Gupta, D. Pathania, S. Agarwal, S. Sharma, Decoloration of hazardous dye from water system using chemically modified *Ficus carica* adsorbent, J. Mol. Liq. 174 (2012) 86–94.
[50] T.K. Sen, S. Afroze, H.M. Ang, Equilibrium, kinetics and mechanism of removal of methylene blue from aqueous solution by adsorption onto pine cone biomass of *Pinus radiate*, Water Air Soil Pollut. 218 (2011) 499–515.
[51] P. Senthil Kumar, S. Ramalingam, C. Senthamarai, M. Niranjanaa, P. Vijayalakshmi, S. Sivanesan, Adsorption of dye from aqueous solution by cashew nut shell: Studies on equilibrium isotherm, kinetics and thermodynamics of interactions, Desalination 261 (2010) 52–60.
[52] W.H. Zou, K. Li, H.J. Bai, X.L. Shi, R.P. Han, Enhanced cationic dyes removal from aqueous solution by oxalic acid modified rice husk, J. Chem. Eng. Data 56 (2011) 1882–1891.
[53] C. Duran, D. Ozdes, A. Gundogdu, H.B. Senturk, Kinetics and isotherm analysis of basic dyes adsorption onto almond shell (*Prunus dulcis*) as a low cost adsorbent, J. Chem. Eng. Data 56 (2011) 2136–2147.
[54] Y.J. Wu, L.J. Zhang, C.L. Gao, J.Y. Ma, X.H. Ma, R.P. Han, Adsorption of copper ions and methylene blue in a single and binary system on wheat straw, J. Chem. Eng. Data 54 (2009) 3229–3234.
[55] P. Senthil Kumar, R.V. Abhinaya, K. Gayathri Lashmi, V. Arthi, R. Pavithra, V. Sathyaselvabala, S. Dinesh Kirupha, S. Sivanesan, Adsorption of methylene blue dye from aqueous solution by agricultural waste: Equilibrium, thermodynamics, kinetics, mechanism and process design, Colloid J. 73 (2011) 651–661.
[56] F. Liu, S. Chung, G. Oh, T. Seok Seo, Three-dimensional graphene oxide nanostructure for fast and efficient water-soluble dye removal, ACS Appl. Mater. Interfaces 4 (2012) 922–927.